Sedimentology of gas hydrate host strata from the JAPEX/JNOC/GSC Mallik 2L-38 gas hydrate research well

K.A. Jenner[1], S.R. Dallimore[2], I.D. Clark[3], D. Paré[4], and B.E. Medioli[2]

Jenner, K.A., Dallimore, S.R., Clark, I.D., Paré, D, and Medioli, B.E., 1999: Sedimentology of gas hydrate host strata from the JAPEX/JNOC/GSC Mallik 2L-38 gas hydrate research well; in *Scientific Results from JAPEX/JNOC/GSC Mallik 2L-38 Gas Hydrate Research Well, Mackenzie Delta, Northwest Territories, Canada, (ed.) S.R. Dallimore, T. Uchida, and T.S. Collett; Geological Survey of Canada, Bulletin 544, p. 57–68.*

Abstract: A detailed sedimentological program has been conducted on gas-hydrate-bearing core samples from the JAPEX/JNOC/GSC Mallik 2L-38 gas hydrate research well. Three structurally and texturally distinct sedimentary facies are identified. Facies Csc (952.2–926.5 m) is a weakly bioturbated, clayey silt interbedded with fissile coal and silty sand. Facies Sg (926.5–908.5 m) is comprised of interbedded, fining-upward successions of matrix-supported gravel to pebbly sand and fine sand. A dolomite-cemented sandstone (926.5–925 m) forms a distinct basal subfacies (Sst). Facies Ss (908.5–886.2 m) is a fine- to medium-grained sand interbedded with gravel which fines upward to fine-grained sand with a gradational increase in silt content. The Kugmallit–Mackenzie Bay sequence boundary is interpreted to occur at the base of facies Sg. In situ and self-preserved gas hydrate occurred mainly in the sands and gravels of the Sg and Ss facies. The dolomite-cemented sandstone (subfacies Sst) may be related to complementary geochemical environments resulting from the formation of authigenic pyrite and solute exclusion related to gas hydrate growth within facies Sg.

Résumé : On a entrepris une étude sédimentologique détaillée d'échantillons carottés renfermant des hydrates de gaz en provenance du puits de recherche sur les hydrates de gaz JAPEX/JNOC/GSC Mallik 2L-38. Trois faciès sédimentaires présentant des structures et des textures distinctes ont été reconnus. Le faciès Csc (de 952,2 à 926,5 m) est un silt argileux faiblement bioturbé, interstratifié de charbon fissile et de sable silteux. Le faciès Sg (de 926,5 à 908,5 m) comporte des séquences interstratifiées à granulométrie décroissante vers le haut qui vont d'un gravier à texture non jointive à du sable caillouteux et à du sable fin. Un grès cimenté par de la dolomie forme un sous-faciès (Sst) distinct à la base de cette succession (de 926,5 à 925 m). Le faciès Ss (de 908,5 à 886,2 m) se compose de sable à grain fin à moyen interstratifié de gravier qui passe à du sable fin dans lequel la teneur en silt augmente progressivement. La base du faciès Sg est interprétée comme étant la frontière entre les séquences de Kugmallit et de Mackenzie Bay. Des hydrates de gaz en place et autoconservés se sont formés principalement dans les sables et graviers des faciès Sg et Ss. Le grès cimenté par de la dolomie (sous-faciès Sst) pourrait être associé à des milieux géochimiques complémentaires formés par suite de la production de pyrite authigène et de l'exclusion de solutes liée à la formation d'hydrates de gaz dans le faciès Sg.

[1] Geological Survey of Canada (Atlantic), P.O. Box 1006, Dartmouth, Nova Scotia B2Y 4A2 Canada
[2] Geological Survey of Canada, 601 Booth Street, Ottawa, Ontario, Canada K1A OE8
[3] Ottawa–Carleton Geoscience Centre, Department of Earth Sciences, University of Ottawa, 140 Louis Pasteur Street, Ottawa, Ontario, Canada K1N 6N5
[4] Consorminex Inc., 11-1695 rue Atmec, Gatineau, Quebec, Canada J8P 7G7

INTRODUCTION

The occurrence of gas hydrate in nature requires specific pressure/temperature conditions, and optimal physical and chemical conditions. Detailed sedimentology is the key to establishing the grain size, mineralogy, salinity, primary porosity, permeability, and depositional history of the gas hydrate host succession. These physical properties exert primary porous media controls on the stability of the in situ gas hydrate and on the processes of heat and mass transfer which may be associated with gas hydrate dissociation or formation. Assessment of the production potential of in situ gas hydrate or evaluation of the sensitivity of gas hydrate to climate change are therefore controlled, in part, by these properties.

The JAPEX/JNOC/GSC Mallik 2L-38 gas hydrate research well was drilled to a depth of 1150 m, at a location on the northeastern edge of the Mackenzie Delta (Fig. 1). As the first research well to investigate a gas hydrate occurrence beneath permafrost, the Mallik 2L-38 well included extensive coring of the gas hydrate interval (Dallimore et al., 1999a; Ohara et al., 1999) and detailed downhole geophysical well logging (Collett et al., 1999b; Miyairi et al., 1999). The resulting data provide a unique opportunity to characterize the sedimentology of gas hydrate host strata. The purpose of this paper is to document gas hydrate host sediments beneath permafrost in Mallik 2L-38 and to propose depositional environments, based on analyses of these strata, which may be favorable for gas hydrate accumulation.

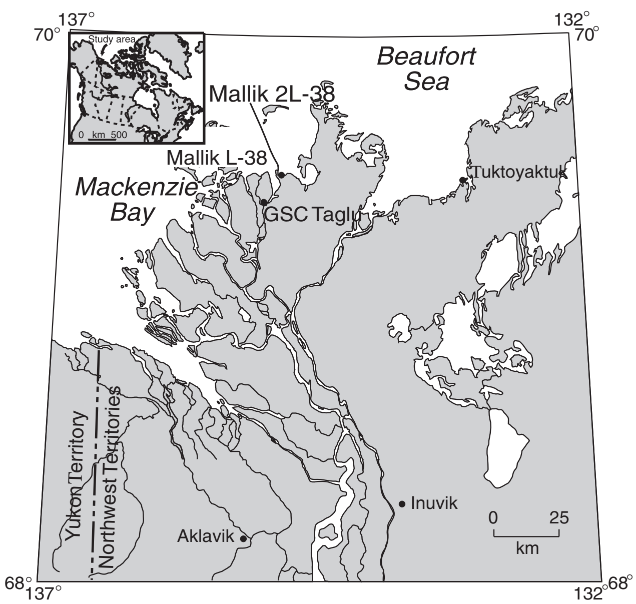

Figure 1. Location map of the Mackenzie Delta region showing the JAPEX/JNOC/GSC Mallik 2L-38 drill site in relation to the Imperial Mallik L-38 and GSC Taglu borehole sites.

GEOLOGICAL SETTING

Lower Cretaceous, highly faulted strata underlie the Mackenzie Delta and form the structural basement for Mackenzie Basin–Beaufort Sea deposits (Dixon et al., 1992). A regional unconformity separates these strata from 12–16 km of Late Cretaceous to Holocene deltaic, shelf, slope, and deep-water deposits of the Mackenzie Basin–Beaufort Sea. Dixon and Dietrich (1988) and Dixon et al. (1992) have subdivided this upper succession into 11 regionally extensive, transgressive-regressive sequences identified from seismic data, well-log data, and to a lesser extent, outcrop information (Fig. 2). This

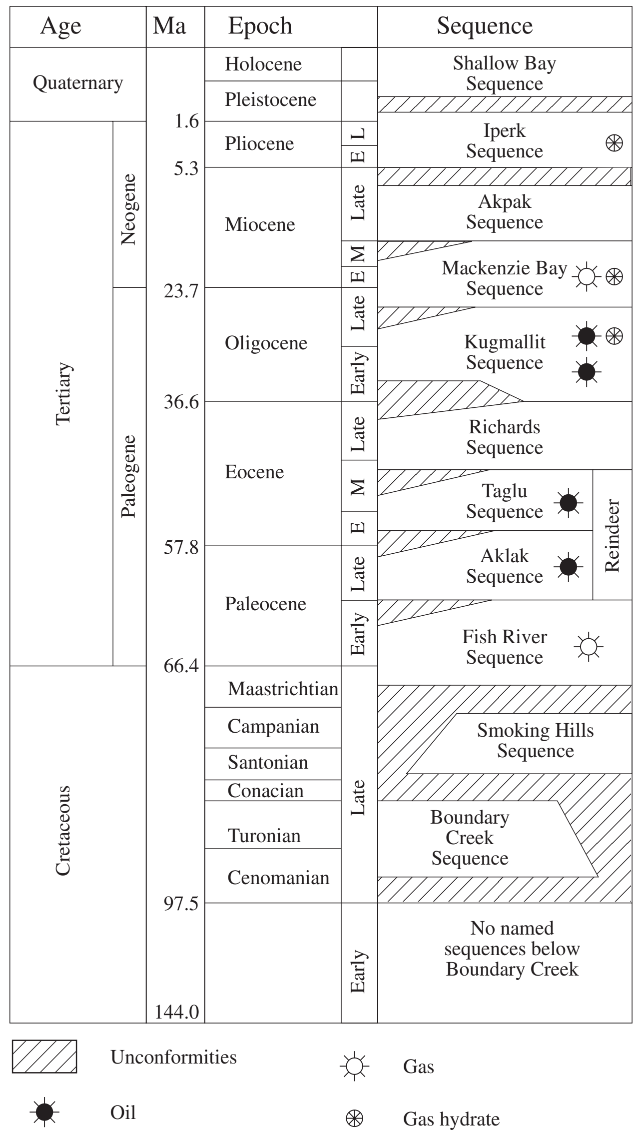

Figure 2. Early Cretaceous to Holocene sequence stratigraphy of the Beaufort Sea–Mackenzie Delta area (modified from Dixon et al. (1992)).

succession is deformed into areally extensive, northwest-trending, linear to curvilinear, thrust-cored folds which originated during periods of Early Eocene to Late Miocene tectonism and compression (Dixon et al., 1992).

Mallik 2L-38 penetrated the upper 1150 m of Oligocene to Holocene sediments. Based on regional seismostratigraphic correlations (Collett et al., 1999a), three of the eleven transgressive-regressive sequences proposed by Dixon and Dietrich (1988) and Dixon et al. (1992) were thought to be intersected. In ascending order, these are the Kugmallit, Mackenzie Bay, and Iperk sequences. Comprehensive, regional descriptions of these sequences are given in Dixon (1986) and Dixon et al. (1992).

LABORATORY METHODOLOGY

Core processing followed a rigorous protocol previously established by the Geological Survey of Canada for arctic drilling programs. Qualitative and quantitative estimates of gas hydrate concentration and preliminary assessment of the core sedimentology were recorded in the field immediately after core retrieval (Dallimore et al., 1999a). Subsamples sensitive to temporal and thermal changes were also collected at the drill site. The core were then cut into 1 m sections, extruded into PVC (polyvinyl chloride) tubing, sealed, and labelled. As described by Wright et al. (1999), most gas-hydrate-bearing core samples were frozen when extruded from the core barrel as a result of endothermic reactions caused by gas hydrate dissociation during core recovery. In contrast, non-gas-hydrate-bearing cores were typically thawed. To prevent any disturbance or contamination, cores were subsequently maintained either frozen or thawed, depending on their recovery state. Approximately five to seven days after initial recovery, core was further processed at the Inuvik Research Centre laboratory. Each 1 m section was split lengthwise, immediately subsampled for moisture content and pore-water analyses, and then photographed with a digital photographic system. One half of the split core underwent detailed sedimentological logging and was archived for future reference; the remaining half was subsampled for a standard suite of analyses. Both split lengths were then wrapped and stored in freezers where they will remain until the year 2000 for further study.

Grain-size analyses of subsamples collected during the sedimentological logging were carried out in the Sedimentology Laboratory at the GSC in Ottawa. The silt and clay fractions were determined using the Galai 2010 particle size analyzer while sand fraction was determined using conventional sieving. Heavy and light mineral determinations were made on the sand fraction of six subsamples by Consorminex Inc. using a binocular microscope equipped with analyzer and nicol. Mineral separations were carried out in methylene iodide (3.3 specific gravity). A dolomite-cemented sandstone, encountered between 926.5 m and 925.0 m (all depths measured from kelly bushing [8.31 m above sea level]), was examined petrographically and isotopically to elucidate the origin of the cement and any potential relationship with the gas hydrate processes in the overlying sand and gravel. Thin sections were prepared from the upper, middle, and lower portions of the sandstone. In addition, subsamples were taken at 10 cm intervals along the core interval and the dolomite cement was analyzed for $\delta^{13}C$ and $\delta^{18}O$. Isotope measurements on CO_2, produced by acidification of the dolomite samples under vacuum with orthophosphoric acid for 48 h, were carried out at the G.G. Hatch Stable Isotope Laboratories, Ottawa, Ontario, Canada.

SEDIMENTOLOGY

Core was recovered from three separate intervals within the Mallik 2L-38 well. Between 109.8 m and 118.4 m, 8.6 m of core were collected; 5 m were collected between 171.0 m and 176.0 m; and 37.3 m of core were recovered from 886.2 m to 952.2 m. The sedimentology of the deepest cored section was associated with a thick gas hydrate interval and provides the basis for this paper.

Three broad sedimentary facies, with distinct sedimentary structures and textures, occur within the basal cored gas hydrate interval of Mallik 2L-38. These sedimentary facies are described below and presented in Figure 3.

Clayey silt and low-rank coal facies (Csc)

The sedimentary succession between 952.2 m and 926.5 m is dominated by massive to weakly laminated, poorly to moderately bioturbated clayey silt and interbedded low-rank coal (Fig. 4a, b, c). Lesser very fine-grained, light grey silty sand is occasionally interlaminated with dark grey silt forming interbeds up to 65 cm thick. Silty sand also occurs as infrequent, massive to weakly laminated, moderately bioturbated beds up to 45 cm thick. Less commonly, angular pebbles (up to 2 mm in diameter) and granules were observed. Fine-grained pyrite was observed within a silt concretion at 936.8 m.

Four separate low-rank coal beds within the silty clay succession range in thickness from 70 mm to a maximum of 400 mm; two of the coal beds are resolvable on the gamma-ray log and deep resistivity laterologs (Fig. 3). Each coal bed displays a distinctive, horizontal fissility at a scale of 1 mm to 10 mm. The coal is very dark brown, breaks apart easily into platy laminae, and leaves a brown residue when scratched. Randomly oriented plant imprints are visible on most fissile surfaces. Basal coal-bed contacts are sharp to gradational over 40 mm; upper contacts are either sharp or gradational into carbonaceous silt (Fig. 4c). These visual coal characteristics are consistent with low-rank lignitic coals.

The relatively massive nature of the clayey silt and the presence of, albeit vague but moderate, organic-rich and sandy burrow infills appears indicative of relatively quiescent marine deposition. The cyclic association of clayey silt and coal suggests that this facies probably represents both marsh and shallow marine deposition in a lower delta-plain environment affected by either fluctuating sediment supply or recurrent changes in relative sea level.

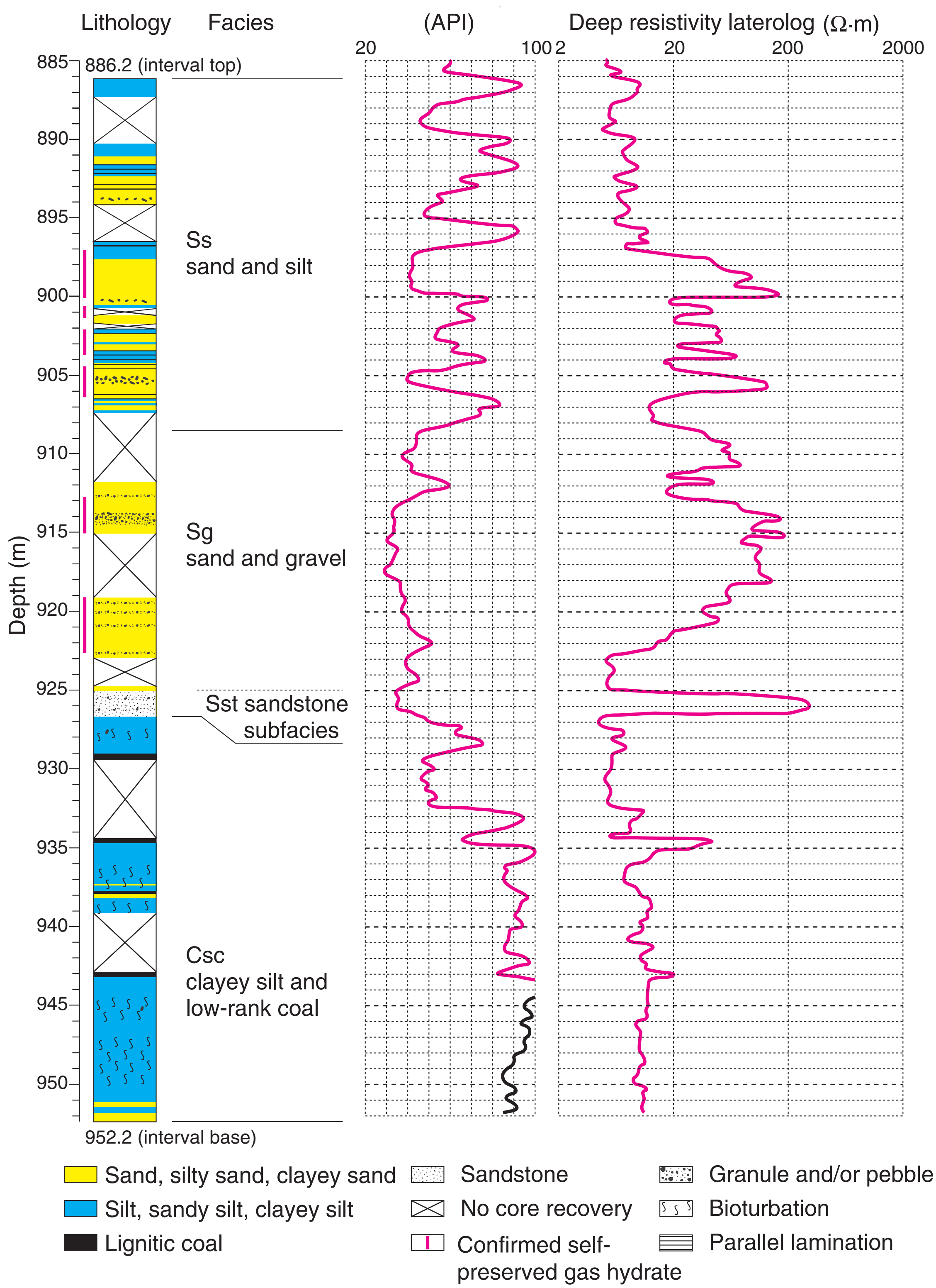

Figure 3. *Lithological log for the gas-hydrate-bearing interval intersected in JAPEX/JNOC/GSC Mallik 2L-38, showing sedimentary facies and the correlation of gamma ray and deep resistivity laterolog responses. The Mackenzie Bay–Kugmallit sequence boundary is interpreted, from sedimentological data, to occur between facies Sst and Csc.*

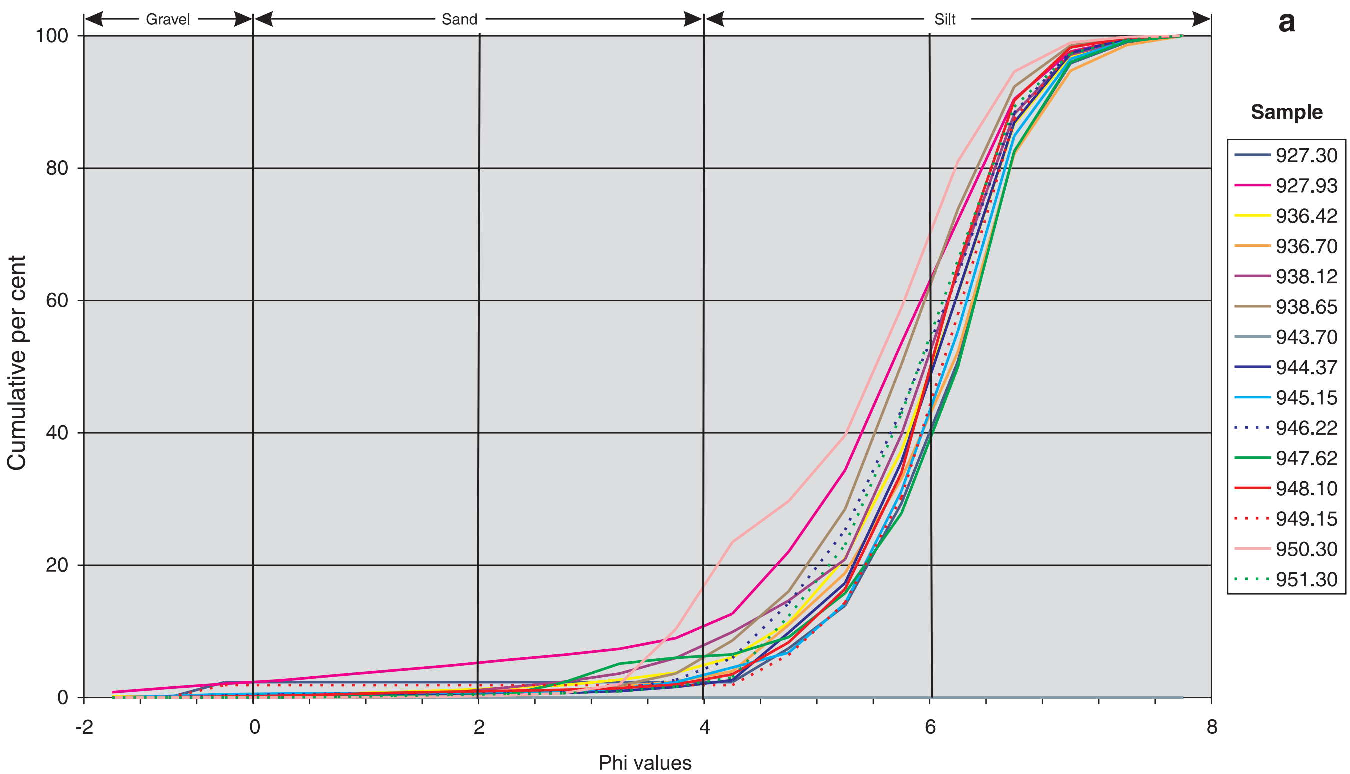

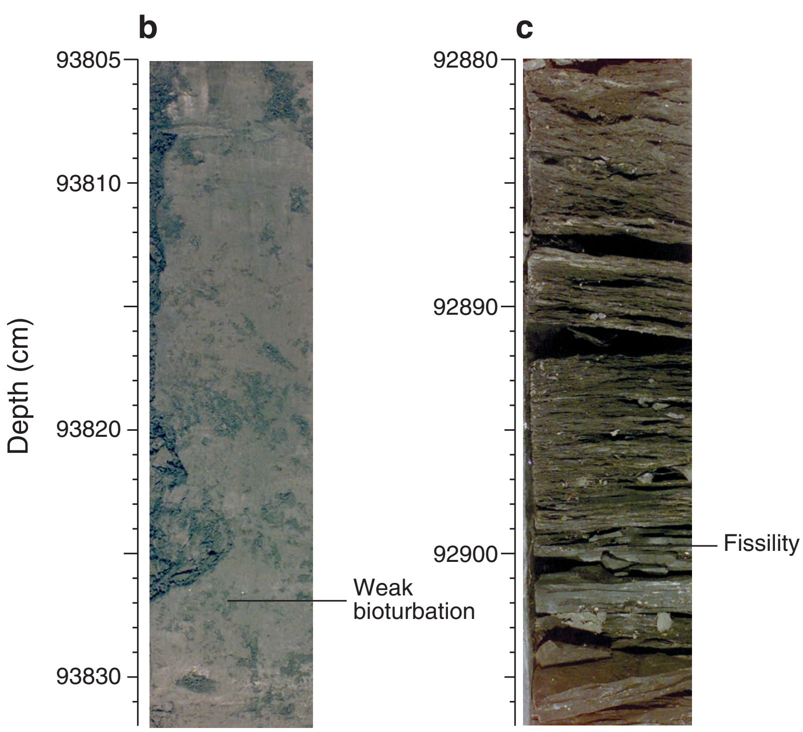

Figure 4.

*Clayey sit and low-rank coal facies, Csc; **a**) cumulative grain-size plots, **b**) massive to weakly bioturbated clayey silt., **c**) basal, low-rank lignitic coal grading upward into carbonaceous silt. The coal and silt display a distinctive, horizontal fissility at a scale of 1 mm to 10 mm.*

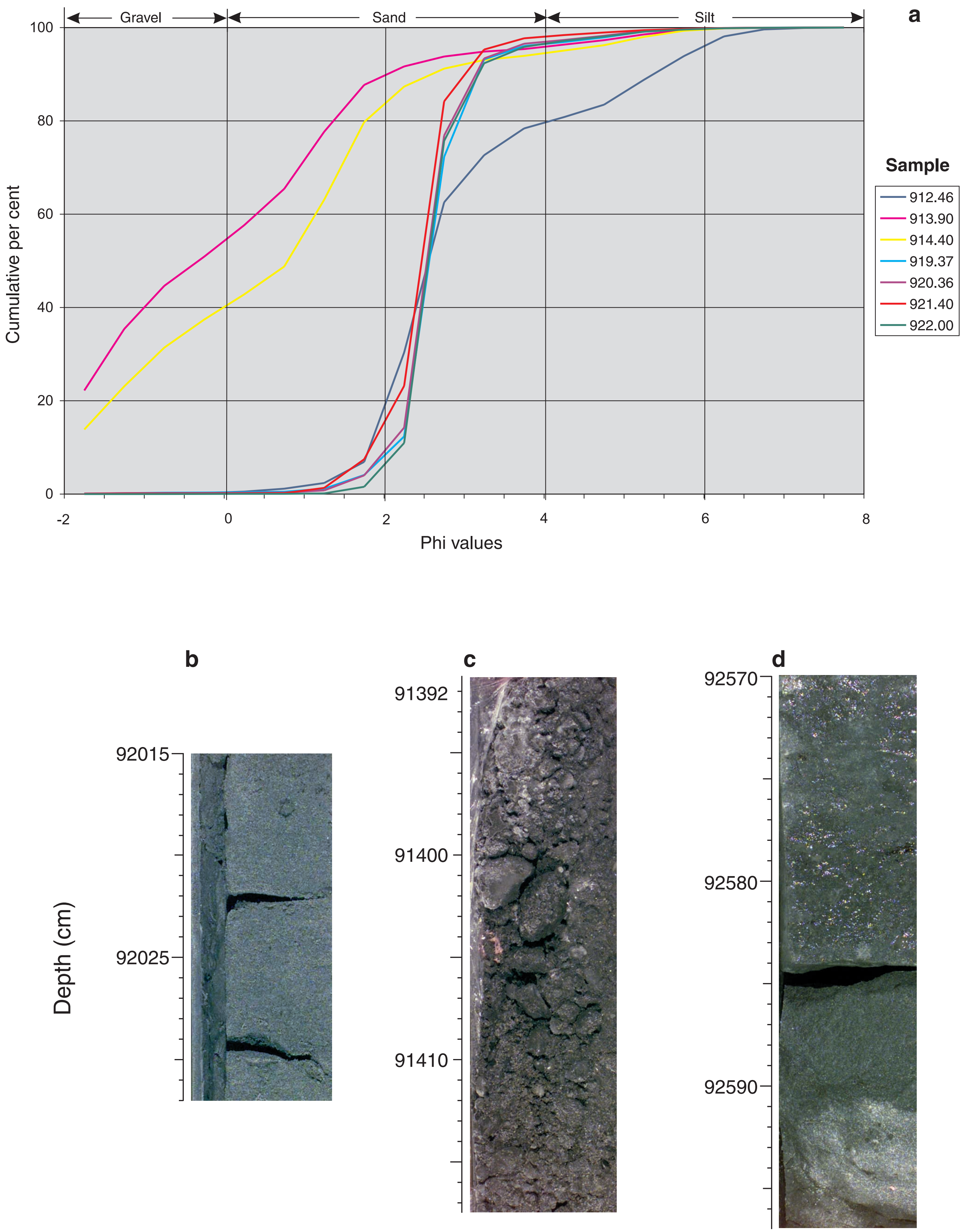
a
Gravel
Sand
Silt
Cumulative per cent
0
20
40
60
80
100
-2
0
2
4
6
8
Phi values
Sample
912.46
913.90
914.40
919.37
920.36
921.40
922.00
b
c
d
Depth (cm)
92015
92025
91392
91400
91410
92570
92580
92590

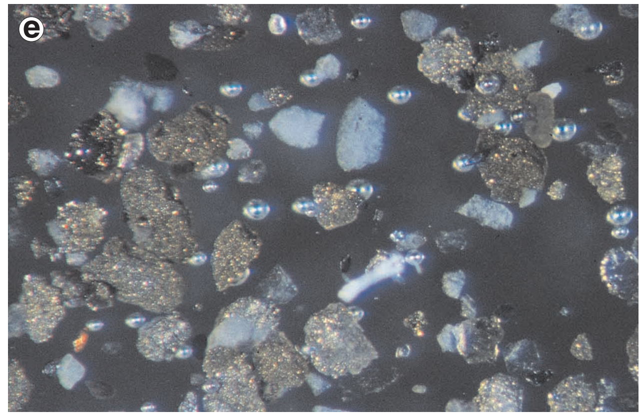

Figure 5.

*Sand and gravel facies, Sg; **a**) cumulative grain-size plots, **b**) well sorted sand with high concentrations of self-preserved gas hydrate, **c**) massive, poorly sorted, sand, granule, and pebble interbed of facies Sg, **d**) dolomite-cemented sandstone of subfacies Sst with rare basal pebbles, **e**) photomicrograph of authigenic pyrite occurring as overgrowths on coal fragments.*

Table 1. Per cent proportion light minerals at the Mallik 2L-38 gas hydrate research well.

Depth (m)	Facies	IN	MU	QZ	Lg	Lb	Ln	CH	UK
921.40	Sg	0.0	0.0	99.3	0.3	0.0	0.3	0.0	0.0
912.46	Sg	0.0	0.0	92.4	4.7	0.0	1.7	1.3	0.0
902.80	Ss	0.3	0.0	83.0	0.7	11.3	0.0	4.3	0.3
898.70	Ss	0.7	0.0	84.3	1.3	12.7	0.3	0.0	0.7
893.10	Ss	1.0	0.7	64.3	0.0	0.0	0.0	33.4	0.7
892.82	Ss	0.7	0.0	85.6	2.7	8.0	0.0	2.0	1.0

Notes: IN=inosilicate; MU=muscovite; QZ=quartz; Lg=lithic fragment, grey; Lb=lithic fragment, brown; Ln=lithic fragment, black; CH=charcoal; UK=unknown or unidentifiable.
<3.3 sg, 63–250 μm, epoxy-cement mounts, 300 grain counts.

Sand and gravel facies (Sg)

The sand and gravel facies occurs between 926.5 m and 908.5 m and is the predominant host strata for gas hydrate. This interval is dominated by well sorted, very fine- to medium-grained sand with infrequent gravel interbeds (Fig. 5a). The sand is primarily massive to faintly parallel laminated; the laminae defined by 5 mm thick concentrations of granules and pebbles or mafic minerals up to 2 mm. Light mineral grains in sands are angular to subangular and dominated by quartz (>90%) with minor lithic fragments and trace amounts of detrital organic material and coal (Table 1). Heavy mineral grains are dominated by pyrite with lesser amounts of barite and trace amounts of garnet, ilmenite, and several other heavy minerals. Pyrite, interpreted to be authigenic in origin, is microcrystalline and typically is attached to, or overgrows detrital coal or other organic material (Fig. 5e). In some instances barite also occurs in contact with pyrite.

Rare silty sand beds occur toward the top of the facies. Several massive gravel interbeds up to 500 mm thick were cored. Gravel beds are predominantly matrix supported, consisting of rounded to subrounded pebbles, fine- to very coarse-grained sand, granules, and rare cobbles (Fig. 5c). Rare, clast-supported gravel was also observed. Basal gravel contacts vary. The limited number of recovered gravel intervals display both erosive and gradational basal contacts with poorly sorted sand.

Although there was insufficient core recovery from this facies to determine vertical trends, the natural gamma ray and resistivity logs clearly show three, 2 m thick fining-up successions; two from gravel to sand and one from gravel to silty sand. These successions resemble several of the detailed fluvial facies presented in Miall (1992). Matrix- and clast-supported gravel is interpreted to have been transported as fluvial bedload. Upward gradation into massive to parallel laminated, very fine- to medium-grained sand with scattered pebbles may represent upper plane bed conditions dominated by traction flow. The presence of silty sand at the top of the upper succession suggests waning flood conditions. Fining-upward successions of pebble-cobble to well sorted, fine- to medium-grained sand and silty sand are interpreted as stacked, fluvial deposits.

Sandstone subfacies (Sst)

The interval between 926.5 m and 925.0 m is similar texturally to the sand and gravel facies but is differentiated by the presence of dolomite cement (Fig. 5d). The sandstone is matrix supported with dolomite infilling the intergranular porosity. No crystallographic faces or rhombohedrons were observed. The degree of cementation toward the base of the sandstone is gradational over 200 mm into partially cemented sandstone and well sorted unconsolidated sand at the base. The basal contact from sand into the underlying clayey silt and low-rank coal facies was disturbed during drilling but is

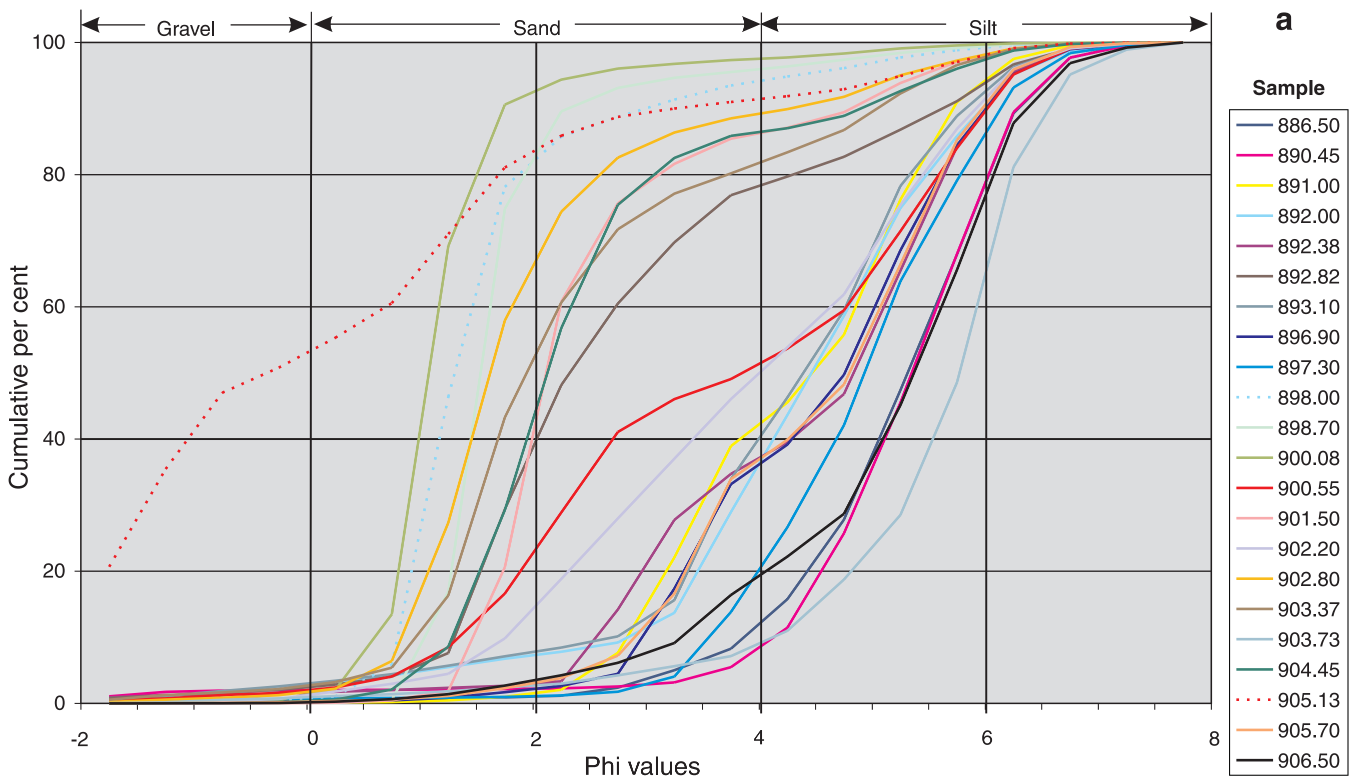

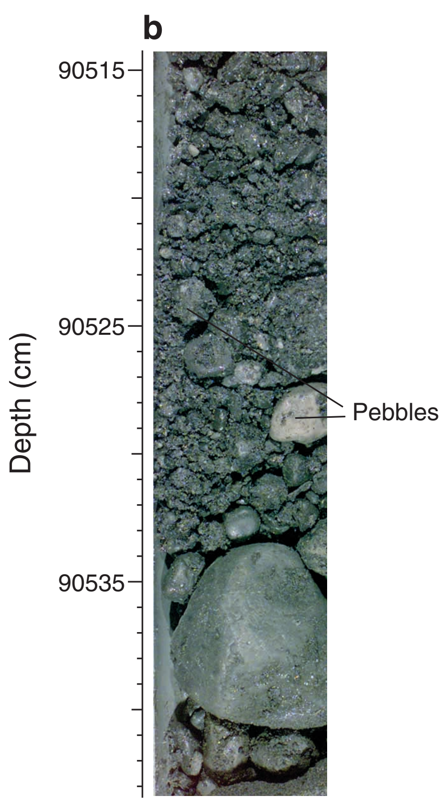

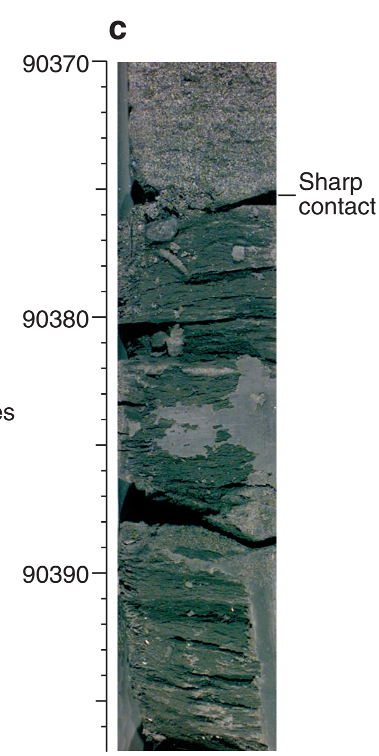

Figure 6.

*Sand and silt facies, Ss; **a**) cumulative grain-size plots, **b**) massive, poorly sorted sand, granule, and pebble bed from facies Ss containing methane hydrate, **c**) interbedded very fine-grained sand and dry, fissile silt and clayey silt of facies Ss. The contact between the sand and silt beds is sharp.*

either sharp or erosional. The upper contact between the sandstone and uncemented sand is sharp. Laminae of fissile carbonaceous material were observed within the sandstone. This material was likely derived from the coal beds observed in the underlying Csc facies. A lamination of microcrystalline pyrite up to 0.5 mm wide and 5 mm long was observed adjacent to the carbonaceous material at one location.

Sand and silt facies (Ss)

This facies occurs from 908.5 m to the top of the cored interval at 886.2 m and contains gas hydrate toward the base of the facies. It is distinguished from the sand and gravel facies by a gradational increase in silt and a concurrent decrease in sand, particularly toward the top of the cored interval (Fig. 6a). Clean, massive, well sorted sand is interbedded with infrequent subangular to subrounded granule and pebble beds up to 500 mm thick, both of which contain gas hydrate (Fig. 6b). The sand is interbedded with distinctly interlaminated, very fine-grained sand; dry, fissile silt; and clayey silt (Fig. 6c). Authigenic pyrite was observed in the silt beds, in some cases acting as a cementing agent (J. Bloch, pers. comm., 1999; *see* Fig. 10c *in* Katsube et al., 1999). The contacts between the sand and silt interbeds are sharp (Fig. 6c). The gradational fining-upward contact between this facies and the basal sand and gravel facies may result from waning flow velocity and progressive channel abandonment or from lateral bar accretion combined with channel aggradation.

The light minerals of three of the four samples investigated from this facies were similar in character to the underlying Sg facies, with a dominance of angular to subangular quartz (>83%) and minor lithic fragments (6–14%). A sample from 893.10 m was also dominated by angular quartz but had 11.7% detrital coal and no lithic fragments (Table 1). The heavy mineralogy was somewhat more variable (Table 2). Microcrystalline pyrite dominated in three of the four samples forming 97.7% of the heavy minerals in the sample from 893.1 m. The abundance of detrital coal from this sample is apparently associated with the pyrite which occurs almost exclusively as authigenic overgrowths on the coal. Barite concentrations in this facies were reduced. Garnet was more variable, making up 53.7% of the sample from 898.7 m but completely absent in the sample from 893.1 m.

DISCUSSION

Gas hydrate host strata

The distribution of gas hydrate is partly controlled by lithology, therefore facies changes are critical to understanding its occurrence. As reviewed in detail in papers by Wright et al. (1999) and Uchida et al. (1999), a distinct characteristic of the Mallik 2L-38 core was the occurrence of frozen gas-hydrate-bearing sands upon recovery. In addition, because of the presence of an ice phase in association with the gas hydrate, the core samples were found to be stable at atmospheric pressures and negative temperatures. This behavior is attributed to the so-called “self preservation phenomena” (Ershove and Yakushev, 1992). Evidence of self-preserved gas hydrate was found in many core samples and was of relevance to the sedimentological program. A qualitative estimate of the relative abundance of self-preserved gas hydrate was determined by immersing frozen sediment samples in water and recording the intensity of degassing. The presence or absence of self-preserved gas hydrate observed during the sedimentological program is shown in Figure 3. Gas hydrate was present in massive, matrix-supported gravel of facies Sg; in massive, well sorted, fine- to medium-grained sand in both facies Sg and facies Ss; and infrequently, in laminated, moderately sorted, silty sand of facies Ss. The most vigorous degassing was observed from coarse pebbly sand and massive, well sorted, fine- to medium-grained sand. Gas hydrate was not observed within interbedded, dry, fissile clayey silt and silt at the top of facies Ss or in the clayey silt of facies Csc at the base of the cored interval.

Sandy and gravelly fluvial deposits seem to have the primary porosity and permeability necessary for gas hydrate concentration in Mallik 2L-38 and Imperial Mallik L-38 (Bily and Dick, 1974). In the channel abandonment succession, particularly within the upper fluvial succession of facies Ss, gas hydrate becomes confined to the coarser sediment fraction and is precluded from finer, thin clayey silt interbeds.

Origin of authigenic pyrite and dolomite cement

The geochemical environment during the formation of authigenic pyrite in sand samples from facies Ss and Sg and observed in thin sections from the dolomite sandstone (subfacies Sst) appears to have been controlled by the occurrence of organic debris (*see* Fig. 5e). Typically organic material can

Table 2. Per cent proportion heavy minerals at the Mallik 2L-38 gas hydrate research well.

Depth (m)	Facies	PY	HM	Hr	IL	Ib	CR	RU	LX	GO	SD	BA	MZ	GA	ZR	KY	ST	CD	EP	OP	Ow	DP	HB	UK
921.40	Sg	38.7	0.7	0.0	2.0	0.0	1.7	0.0	0.7	0.0	0.0	21.7	0.3	14.7	0.7	0.0	1.3	0.7	3.3	8.0	0.0	0.3	2.0	3.0
912.46	Sg	59.0	1.7	1.0	6.3	0.0	0.0	0.0	0.3	0.3	0.0	22.0	0.0	5.7	0.7	0.0	0.0	0.0	0.3	1.0	0.0	0.0	0.7	1.0
902.80	Ss	70.6	0.0	0.0	0.3	0.0	0.3	0.3	1.3	0.0	0.0	10.0	0.0	8.7	0.3	0.0	0.7	0.3	1.7	2.3	0.0	0.3	0.7	2.0
898.70	Ss	25.3	0.0	0.0	0.0	0.0	0.3	0.0	0.0	0.0	0.3	4.7	0.0	53.7	0.0	1.0	6.3	0.0	4.0	0.7	0.0	0.0	0.0	3.7
893.10	Ss	97.7	0.0	0.0	0.0	0.0	0.0	0.0	0.0	0.0	0.0	1.7	0.0	0.0	0.0	0.0	0.0	0.0	0.0	0.3	0.0	0.0	0.0	0.3
892.82	Ss	69.0	0.0	0.0	1.0	0.5	0.0	0.3	0.0	0.0	0.0	9.7	0.0	9.3	0.3	0.0	0.3	0.3	1.0	1.0	0.3	0.0	0.0	2.3

Notes: PY=pyrite, multi-crystalline; HM=hematite, grey; Hr=Hematite, red; IL=ilmenite, grey; Ib=ilmenite, black; CR=chromite; RU=rutile; LX=leucoxene; GO=goethite; SD=siderite; BA=barite; MZ=monazite; GA=garnet; ZR=zircon; KY=kyanite; ST=staurolite; CD=chloritoid; EP=epidote; OP=orthopyroxene; Ow=hypersthene, weathered; DP=diopside; HB=hornblende; UK=unknown or unidentifiable.
<3.3 sg, 63–250 µm, Araldite mounts, 300 grain counts.

maintain low redox conditions in the pore waters. If one assumes that a significant component of the contemporary pore waters was seawater then up to 2700 mg/L of SO_4^{2-} would have been available for oxidation of organic material. Low redox potentials accompanying sulphate reduction could have reduced ferric iron sources such as limonite and goethite.

Oxidation of fixed carbon sources such as plant debris proceeds via the following reaction:

$$CH_2O + 2H_2O \rightarrow HCO_3^- + 4e^- + 5H^+ \qquad (1)$$

where CH_2O represents organic matter. In the absence of elemental oxygen, other electron acceptors such as sulphate and ferric iron minerals will be reduced in a complementary reduction reaction. For dissolved sulphate and goethite, bacteria will mediate reactions similar to:

$$FeOOH + 2\,SO_4^{2-} + 19H^+ + 15e^- \rightarrow FeS_2 + 10\,H_2O \qquad (2)$$

The net reaction would then be:

$$3\tfrac{3}{4}CH_2O + FeOOH + 2\,SO_4^{2-} + \tfrac{1}{4}H^+ \rightarrow FeS_2 + 3\tfrac{3}{4}HCO_3^- + 2\tfrac{1}{2}H_2O \qquad (3)$$

Two important effects of this overall reaction are the consumption of H^+, which increases pore-water pH, and the production of inorganic carbon (HCO_3^- and CO_3^{2-}). Accordingly, precipitation of carbonate minerals will be favoured. Dolomite is known to form in environments of elevated Mg^{2+} concentrations and Mg/Ca ratios (Baker and Kastner, 1981). A source of dissolved carbonate and alkaline pH conditions are also essential, allowing dolomite precipitation according to:

$$Mg^{2+} + Ca^{2+} + 2\,CO_3^{2-} \rightarrow MgCa(CO_3)_2 \qquad (4)$$

Investigation of the geochemistry of pore waters in Mallik 2L-38 has confirmed that formation of gas hydrate, in the sands of facies Sg which overlie the dolomite-cemented sandstone, was accompanied by solute expulsion (Cranston, 1999; Clark et al., 1999) and increased salinity of the residual pore fluids. This would increase the Mg^{2+} concentration of the pore fluids at the base of the gas hydrate sands. Contemporaneous sulphate reduction throughout the section would produce a carbonate-rich pore fluid from the oxidation of sedimentary organic debris. Furthermore, this fluid would be depleted in sulphate which can inhibit formation of dolomite. Mixing at the interface of these two zones would then favour the precipitation of dolomite. It is probably for this reason that the dolomite cement only occurs at the base of the gas-hydrate-bearing sands.

This scenario is supported by stable isotope analysis of the dolomite cements. Figure 7 is a profile of $\delta^{13}C$ and $\delta^{18}O$ in the dolomite-cemented sandstone. It shows only minor variation in $\delta^{13}C$ (average = –13.5 ± 1.1‰) and even less variation for $\delta^{18}O$ (average $\delta^{18}O$ = 0.6 ± 0.34‰). The low $\delta^{13}C$ values demonstrate that the dolomite cements rely on an organic carbon source for a portion of their carbonate. Seawater carbonate has a $\delta^{13}C$ value close to 0, while vegetation is

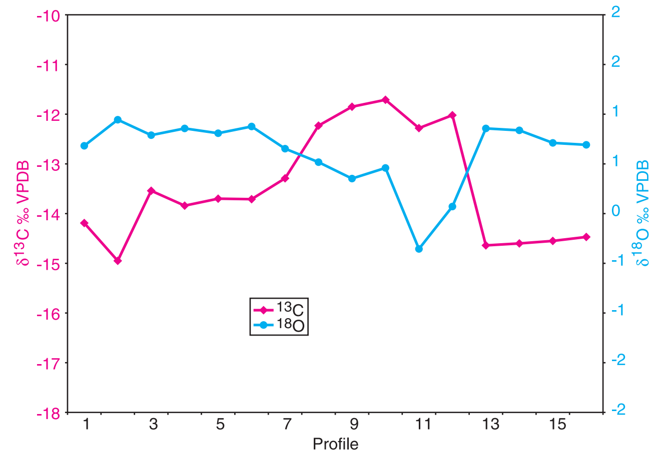

Figure 7. *Profile of $\delta^{13}C$ and $\delta^{18}O$ through dolomite-cemented sandstone. VPDB = Vienna Pee Dee Belemnite.*

characterized by $\delta^{13}C$ values of -25‰ to -30‰. A simple carbon mass balance would suggest that about half of the carbonate came from sulphate reduction.

The $\delta^{18}O$ composition of the dolomite records the pore-water composition during dolomite precipitation. Using the average value of 0.6‰, and assuming a formation temperature in the order of 6°C during gas hydrate formation, the pore water would have had a $\delta^{18}O$ value of about –8‰ (VSMOW; Vienna Standard Mean Ocean Water). This estimate is not well constrained due to uncertainties in establishing the dolomite-water fractionation factor at low temperature, and is based on the fractionation factors of Northrop and Clayton (1966) and O'Neil and Epstein (1966). Using the fractionation factor of Fritz and Smith (1970) provides an average value of –4.3‰ VSMOW. Despite the uncertainties, these data indicate that the original pore waters were dominantly marine with some contribution by continental runoff.

Mallik 2L-38 preliminary stratigraphic summary

A stratigraphic framework in the vicinity of Mallik L38 and 2L-38 well sites, based on seismic reflection profiles and geophysical well-log data, was given in Dixon et al. (1992), Dixon (1995), and Collett et al. (1999a). These interpretations suggest that the Kugmallit, Mackenzie Bay, and Iperk sequences should have been encountered within the upper 1150 m. While these data provide general constraints on the sequence boundaries it is difficult to assign specific depths as the seismic lines do not intersect the Mallik well sites and biostratigraphic data was limited prior to the Mallik 2L-38 drilling program.

Based on facies identification, Kugmallit Sequence strata in Mallik 2L-38 are interpreted to begin at 926.5 m at the base of sandstone subfacies Sst — which is also the contact between facies Csc and facies Sg — and to continue to the bottom of the borehole (Fig. 3). This is similar to the depth of 935 m estimated at Mallik L-38 by Dallimore and Collett

(1999) on the basis of well-log response, but deeper than the depth of 868 m estimated by J. Dixon (pers. comm., 1998) on the basis of regional biostratigraphic evidence. Unfortunately, detailed paleontological analyses carried out on core samples from Mallik 2L-38 in the interval from 890–953 m (Kurita and Uchida, 1999; McNeil, 1999; White, 1999) have not conclusively resolved the age of the strata or the position of the boundary primarily because of concerns over the presence of reworked fossil indicators (*see* ‘Summary’ *in* Dallimore et al., 1999b). Based solely on the sedimentological evidence cited in this paper, the Kugmallit–Mackenzie Bay sequence boundary in Mallik 2L-38 is suggested to occur at 926.5 m. As a result, the upper gas hydrate interval would lie fully within the Late Oligocene to Early Miocene Mackenzie Bay Sequence.

The upper contact of the Kugmallit Sequence with the overlying Late Oligocene to Middle Miocene Mackenzie Bay Sequence is abrupt but conformable (Dixon, 1986). Well-log data from the Mallik 2L-38 well indicate that the Mackenzie Bay Sequence consists predominantly of sand with silt interbeds, particularly toward the base of the sequence, with an overall fining-upward trend into clayey silt toward the top of the sequence. Gas hydrate occurs at the base of the Mackenzie Bay Sequence within coarser sand interbeds. The subordinate silt and finer sediment fraction supports a localized facies change at Mallik 2L-38 from regional, fine prodelta slope and deep-water deposits with sand-rich interbeds characteristic of the Mackenzie Bay Sequence, to atypical coarser sands. This facies change was also noted by Dixon et al. (1992) in several other Mallik boreholes.

The Iperk–Mackenzie Bay sequence boundary has been interpreted to occur at Mallk 2L-38 at 346 m (Dallimore et al., 1999a). A similar gamma-ray response at approximately 350 m in Mallik L-38 has been interpreted as the Miocene–Pliocene erosional unconformity separating lower, fining-upward Mackenzie Bay Sequence strata from relatively coarser Iperk Sequence strata (J. Dixon, pers. comm., 1998). The Akpak Sequence, which lies further offshore, is absent in the Mallik 2L-38 well (Dixon et al., 1992). Core material and geophysical log responses from Mallik 2L-38 record a predominantly sand-dominated Iperk Sequence with gravel interbeds and infrequent detrital woody beds. Regionally, the landward part of the Iperk Sequence consists of fluvial sand and gravel which grades offshore into a deltaic succession of sand and silt (Dixon et al., 1992).

CONCLUSIONS

The Mallik 2L-38 research well provided a unique opportunity to investigate the sedimentology of the gas hydrate host strata, and ascertain the relationships between gas hydrate occurrence and sedimentary depositional environments. Thirty-seven metres of core were recovered between 886 m and 952 m and characterize the gas-hydrate-bearing interval. These sediments are interpreted to be part of the Early Miocene to Late Oligocene, Lower Mackenzie Bay and Upper Kugmallit sequences. The cored interval can be subdivided, on the basis of lithology, into three distinct facies and one subfacies. A clayey silt and low-rank coal facies (Csc) consists of a sedimentary succession, from 952.2 m to 926.5 m, that is dominated by weakly bioturbated clayey silt with thin interbeds of low-rank, fissile coal and silty sand. On the basis of the sedimentology, this facies is interpreted to represent both marsh and shallow-marine deposition in a lower delta-plain environment. A sand and gravel facies (Sg) that occurs from 926.5 m to 908.5 m consists of well sorted, fine- to medium-grained sand with infrequent gravel interbeds and rare silty sand beds. A dolomite-cemented sandstone occurring at the base of the Csc facies, from 926.5 m to 925.0 m, is considered a subfacies (Sst). Finally, from 908.5 m to 886.2 m, a sand-dominated facies (Ss) is comprised of a succession of basal fine- to medium-grained sand and interbedded gravel fining upward into fine sand with a gradational increase in silt content. Facies Sg and Ss are interpreted to be deposited in a fluvial environment with variable flow conditions. On the basis of the sedimentological character of the cored succession, the Kugmallit–Mackenzie Bay sequence boundary in Mallik 2L-38 is interpreted to occur at 926.5 m — the base of the dolomite-cemented sandstone.

In addition to various visible forms of gas hydrate observed at the drill site, pore-space gas hydrate was recorded during the sedimentological logging program. The stability of gas hydrate, at atmospheric pressures some five to seven days after core retrieval, is attributed to the self-preservation effect whereby gas hydrate dissociation is retarded by the presence of an ice coating. The highest gas hydrate concentrations occurred in the matrix-supported gravel and well sorted, fine- to medium-grained sands of facies Sg and Ss. Gas hydrate was less abundant in the laminated, moderately sorted, silty sand of facies Ss and was absent from facies Csc.

Authigenic pyrite, in association with detrital coal and organic material, was observed in each facies. This suggests an active postdepositional geochemical environment characterized by alkaline pore fluids with elevated dissolved carbonate of organic origin. The dolomite-cemented sandstone may have occurred as a consequence of complementary geochemical environments within facies Sg. Gas hydrate formation in the overlying sands would have generated downward migrating pore waters with high salinity and elevated Mg^{2+}. Diffusional mixing of these migrating pore waters and waters associated with the formation of the authigenic pyrite may have been responsible for precipitation of dolomite cement at the base of the sands in this zone.

ACKNOWLEDGMENTS

In addition to the considerable support given by the chief scientists for the Mallik 2L-38 research program, the authors wish to acknowledge the Polar Continental Shelf Project and the Inuvik Research Centre for outstanding logistical support during the fieldwork — in particular Jerry McEachern and Les Kutny. Bob Harmes and Richard Laframboise provided exceptional technical expertise toward the sedimentological field program. The authors appreciate critical reviews of an early version of the paper by David Piper and Ray Cranston. The paper was enhanced through discussions with Tim Collett, John Katsube, Mark Nixon, William Winters, and Takashi Uchida. Grain-size analyses were completed under the direction of Miriam Wygergangs in Ottawa. Ken Hale generated the figures.

REFERENCES

Baker, P.A. and Kastner, M.
1981: Constraints on the formation of sedimentary dolomite; Science, v. 213, p. 214–216.

Bily, C. and Dick, J.W.L.
1974: Naturally occurring gas hydrates in the Mackenzie Delta, N.W.T; Bulletin of Canadian Petroleum Geology, v. 22, p. 340–352.

Clark, I.D., Matsumoto, R., Dallimore, S.R., Lowe, B., and Loop, J.
1999: Isotope constraints on the origin of pore waters and salinity in the permafrost and gas hydrate core intervals of the JAPEX/JNOC/GSC Mallik 2L-38 gas hydrate research well; *in* Scientific Results from JAPEX/JNOC/GSC Mallik 2L-38 Gas Hydrate Research Well, Mackenzie Delta, Northwest Territories, Canada, (ed.) S.R. Dallimore, T. Uchida, and T.S. Collett; Geological Survey of Canada, Bulletin 544.

Collett, T.S., Lee, M.W., Dallimore, S.R., and Agena, W.F.
1999a: Seismic- and well-log-inferred gas hydrate accumulations on Richards Island; *in* Scientific Results from JAPEX/JNOC/GSC Mallik 2L-38 Gas Hydrate Research Well, Mackenzie Delta, Northwest Territories, Canada, (ed.) S.R. Dallimore, T. Uchida, and T.S. Collett; Geological Survey of Canada, Bulletin 544.

Collett, T.S., Lewis, R., Dallimore, S.R., Lee, M.W., Mroz, T.H., and Uchida, T.
1999b: Detailed evaluation of gas hydrate reservoir properties using JAPEX/JNOC/GSC Mallik 2L-38 gas hydrate research well downhole well-log displays; *in* Scientific Results from JAPEX/JNOC/GSC Mallik 2L-38 Gas Hydrate Research Well, Mackenzie Delta, Northwest Territories, Canada, (ed.) S.R. Dallimore, T. Uchida, and T.S. Collett; Geological Survey of Canada, Bulletin 544.

Cranston, R.E.
1999: Pore-water geochemistry, JAPEX/JNOC/GSC Mallik 2L-38 gas hydrate research well; *in* Scientific Results from JAPEX/JNOC/GSC Mallik 2L-38 Gas Hydrate Research Well, Mackenzie Delta, Northwest Territories, Canada, (ed.) S.R. Dallimore, T. Uchida, and T.S. Collett; Geological Survey of Canada, Bulletin 544.

Dallimore, S.R. and Collett, T.S.
1999: Regional gas hydrate occurrences, permafrost conditions, and Cenozoic geology, Mackenzie Delta area; *in* Scientific Results from JAPEX/JNOC/GSC Mallik 2L-38 Gas Hydrate Research Well, Mackenzie Delta, Northwest Territories, Canada, (ed.) S.R. Dallimore, T. Uchida, and T.S. Collett; Geological Survey of Canada, Bulletin 544.

Dallimore, S.R., Collett, T.S., and Uchida, T.
1999a: Overview of science program, JAPEX/JNOC/GSC Mallik 2L-38 gas hydrate research well; *in* Scientific Results from JAPEX/JNOC/GSC Mallik 2L-38 Gas Hydrate Research Well, Mackenzie Delta, Northwest Territories, Canada, (ed.) S.R. Dallimore, T. Uchida, and T.S. Collett; Geological Survey of Canada, Bulletin 544.
1999b: Scientific Results from JAPEX/JNOC/GSC Mallik 2L-38 Gas Hydrate Research Well, Mackenzie Delta, Northwest Territories, Canada, (ed.) S.R. Dallimore, T. Uchida, and T.S. Collett; Geological Survey of Canada, Bulletin 544.

Dixon, J.
1986: Cretaceous to Pleistocene stratigraphy and paleography, northern Yukon and northwestern District of Mackenzie; Bulletin of Canadian Petroleum Geology, v. 34, p. 49–70.
1995: Geological Atlas of the Beaufort – Mackenzie area. Geological Survey of Canada, Miscellaneous Report 59, 173 p.

Dixon, J. and Dietrich, J.R.
1988: The nature of depositional and seismic sequence boundaries in Cretaceous–Tertiary strata of the Beaufort – Mackenzie Basin; *in* Sequences, Stratigraphy, Sedimentology: Surface and Subsurface, (ed.) D.P. James and D.A. Leckie; Canadian Society of Petroleum Geologists, Memoir 15, p. 63–72.

Dixon, J., Dietrich, J.R., and McNeil, D.H.
1992: Upper Cretaceous to Pleistocene sequence stratigraphy of the Beaufort–Mackenzie and Banks Island areas, northwest Canada; Geological Survey of Canada, Bulletin 407, 90 p.

Ershov, E.D. and Yakushev, V.S.
1992: Experimental research on gas hydrate decomposition in frozen rocks; Cold Regions Science and Technology, v. 20, p. 147–156

Fritz, P. and Smith, D.C.W.
1970: The isotopic composition of secondary dolomites; Geochimica Cosmochimica Acta, v. 34, p. 1161–1173.

Katsube, T.J., Dallimore, S.R., Uchida, T., Jenner, K.A., Collett, T.S., and Connell, S.
1999: Petrophysical environment of sediments hosting gas hydrate, JAPEX/JNOC/GSC Mallik 2L-38 gas hydrate research well; *in* Scientific Results from JAPEX/JNOC/GSC Mallik 2L-38 Gas Hydrate Research Well, Mackenzie Delta, Northwest Territories, Canada, (ed.) S.R. Dallimore, T. Uchida, and T.S. Collett; Geological Survey of Canada, Bulletin 544.

Kurita, H. and Uchida, T.
1999: Dinoflagellate cysts from the JAPEX/JNOC/GSC Mallik 2L-38 gas hydrate research well; *in* Scientific Results from JAPEX/JNOC/GSC Mallik 2L-38 Gas Hydrate Research Well, Mackenzie Delta, Northwest Territories, Canada, (ed.) S.R. Dallimore, T. Uchida, and T.S. Collett; Geological Survey of Canada, Bulletin 544.

McNeil, D.H.
1999: Micropaleontology of the JAPEX/JNOC/GSC Mallik 2L-38 gas hydrate research well; *in* Scientific Results from JAPEX/JNOC/GSC Mallik 2L-38 Gas Hydrate Research Well, Mackenzie Delta, Northwest Territories, Canada, (ed.) S.R. Dallimore, T. Uchida, and T.S. Collett; Geological Survey of Canada, Bulletin 544.

Miall, A.D.
1992: Alluvial deposits; *in* Facies Models Response to Sea Level Change, (ed.) R.G. Walker and N.P. James; Geological Association of Canada, p. 119–142.

Miyairi, M., Akihisa, K., Uchida, T., Collett, T.S., and Dallimore, S.R.
1999: Well-log interpretation of gas-hydrate-bearing formations in the Mallik 2L-38 gas hydrate research well; *in* Scientific Results from JAPEX/JNOC/GSC Mallik 2L-38 Gas Hydrate Research Well, Mackenzie Delta, Northwest Territories, Canada, (ed.) S.R. Dallimore, T. Uchida, and T.S. Collett; Geological Survey of Canada, Bulletin 544.

Northrop, D.A. and Clayton, R.N.
1966: Oxygen isotope composition of the oceanic crust and its bearing on seawater; Journal of Geophysical Research, v. 81, p. 4362–4369.

Ohara, T., Dallimore, S.R., and Fercho, E.
1999: Drilling operations, JAPEX/JNOC/GSC Mallik 2L-38 gas hydrate research well; *in* Scientific Results from JAPEX/JNOC/GSC Mallik 2L-38 Gas Hydrate Research Well, Mackenzie Delta, Northwest Territories, Canada, (ed.) S.R. Dallimore, T. Uchida, and T.S. Collett; Geological Survey of Canada, Bulletin 544.

O'Neil, J.R. and Epstein, S.
1966: Oxygen isotope fractionation in the system dolomite-calcite-carbon dioxide; Science, v. 152, p. 198–201.

Uchida, T., Dallimore, S.R., Mikami, J., and Nixon, F.M.
1999: Occurrences and X-ray computerized tomography (CT) observations of natural gas hydrate, JAPEX/JNOC/GSC Mallik 2L-38 gas hydrate research well; *in* Scientific Results from JAPEX/JNOC/GSC Mallik 2L-38 Gas Hydrate Research Well, Mackenzie Delta, Northwest Territories, Canada, (ed.) S.R. Dallimore, T. Uchida, and T.S. Collett; Geological Survey of Canada, Bulletin 544.

White, J.
1999: Palynology, age, and paleoenvironmental interpretations from the JAPEX/JNOC/GSC Mallik 2L-38 gas hydrate research well; *in* Scientific Results from JAPEX/JNOC/GSC Mallik 2L-38 Gas Hydrate Research Well, Mackenzie Delta, Northwest Territories, Canada, (ed.) S. R. Dallimore, T. Uchida, and T. S. Collett; Geological Survey of Canada, Bulletin 544.

Wright, J.F., Taylor, A.E., Dallimore, S.R., and Nixon, F.M.
1999: Estimating in situ gas hydrate saturation from core temperature observations, JAPEX/JNOC/GSC Mallik 2L-38 gas hydrate research well; *in* Scientific Results from JAPEX/JNOC/GSC Mallik 2L-38 Gas Hydrate Research Well, Mackenzie Delta, Northwest Territories, Canada, (ed.) S.R. Dallimore, T. Uchida, and T.S. Collett; Geological Survey of Canada, Bulletin 544.